# International Conference on Space Optics—ICSO 2014

La Caleta, Tenerife, Canary Islands

7–10 October 2014

## *Towards a fully integrated optical gyroscope using whispering gallery modes resonators*

*T. Amrane*

*J.-B., CEA Jager*

*T. Jager*

*V., CEA Calvo*

*et al.*

# TOWARDS A FULLY INTEGRATED OPTICAL GYROSCOPE USING WHISPERING GALLERY MODES RESONATORS

T. Amrane[a1], J.-B. Jager[2], T. Jager[1], V. Calvo[2] and J.M. Léger[1]

[1]Univ. Grenoble Alpes, F-38000 Grenoble, France
CEA, LETI, MINATEC Campus, F-38054 Grenoble, France.
[2]CEA, INAC-SP2M / SiNaPS, F-38000 Grenoble, France.

## I. INTRODUCTION

Since the developments of lasers and the optical fibers in the 70s, the optical gyroscopes have been subject to an intensive research to improve both their resolution and stability performances [1-4]. However the best optical gyroscopes currently on the market, the ring laser gyroscope and the interferometer fiber optic gyroscope are still macroscopic devices and cannot address specific applications where size and weight constraints are critical. One solution to overcome these limitations could be to use an integrated resonator as a sensitive part to build a fully Integrated Optical Resonant Gyroscope (IORG). To keep a high rotation sensitivity, which is usually degraded when downsizing this kind of optical sensors based on the Sagnac effect, the resonator has to exhibit a very high quality factor ($Q$): as detailed in equation (1) where the minimum rotation rate resolution for an IORG is given as a function of the resonator characteristics ($Q$ and diameter $D$) and of the global system optical system characteristics (i.e. $SNR$ and bandwidth $B$), the higher the $Q{\times}D$ product, the lower the resolution.

$$\delta\Omega_{min} = \frac{c\sqrt{2}}{QD} \times \frac{\sqrt{B}}{SNR} \qquad \text{where c is the speed of light in vacuum (1)}$$

The research for new integrated resonators has generated important efforts in the last decade and several designs have been tested to achieve the first prototype of a high performances IORG. The most common design is the integrated $SiO_2$ ring resonator used by Ma [5][6] thanks to which a theoretical minimum rotation rate resolution of 17 °/h has been achieved. The resonator used by Hotate and Lei [7-9], a square waveguide with rounded corners, is the resonator with the highest quality factor ($3.9{\times}10^6$) used to date as a sensitive part of an IORG, with a theoretical resolution of 1.4 °/h. However most of the aforementioned resonator designs have a diameter of few centimeters. In order to increase further the sensor downsizing, $SiO_2$ microdisk Whispering Gallery Modes Resonators (WGMR) may be advantageously used. This type of resonators has already demonstrated quality factors several orders of magnitude higher than the ones currently achieved with the previous structures used in IORG [10]. Thanks to their ultra-high-Q, a rotation rate resolution as low as 0.2 °/h with a size lowered by a factor of 10 with respect to previous structures could be achieved.

In this paper, we present our preliminary results towards using $SiO_2$ microdisk WGMR as the sensitive part of an IORG. These resonators have been specifically designed and fabricated in order to achieve the highest possible $Q{\times}D$ product. Stand-alone resonator characterizations results are presented: they currently demonstrate $Q{\times}D$ values at the state of the art previously mentioned, with a remaining potential improvement of one to two orders of magnitude. A specific low refractive index polymer packaging is also detailed and assessed, as it is mandatory to ensure a protective packaging and a stable optical coupling between the resonator and the optical circuit for any rotation testing. First steps towards system level characterization are also presented.

## II. REALIZATION AND CHARACTERIZATION OF DEDICATED SiO2 MICRODISKS RESONATORS

Disks with diameters in the [100 µm – 5 mm] range have been fabricated on a <100> silicon substrate by standard microelectronic processing methods [10-11]. The process flow begins with the growth of a 3 µm thick silica layer by wet thermal oxidation of the substrate. Circular photoresist pads are then defined by optical lithography on the silica layer. The patterned disks are transferred to the silica by wet etching in buffered hydrofluoric solution. After removing photoresist by conventional cleaning process, silicon is isotropically etched by a fluorine chemistry ($SF_6$/Ar plasma) in an ICP-RIE tool to create a silica disk on a silicon pillar with high Q whispering gallery modes. Inspired by the work of the Vahala research group [10] we have improved our process flow to reduce the surface roughness at the edge of the silica disk and a dry oxidation step was added to reduce optical losses in the silica layer. An example of realization is given on Fig.1.a, where a SEM picture of a 400 µm diameter $SiO_2$ microdisk is shown. The effect of the specific roughness optimization steps is illustrated on Fig.1.b and Fig.1.c, where a standard $SiO_2$ disk edge interface roughness is shown on the disk A of Fig.1.b, and an optimized one is shown on the disk B on Fig.1.c.
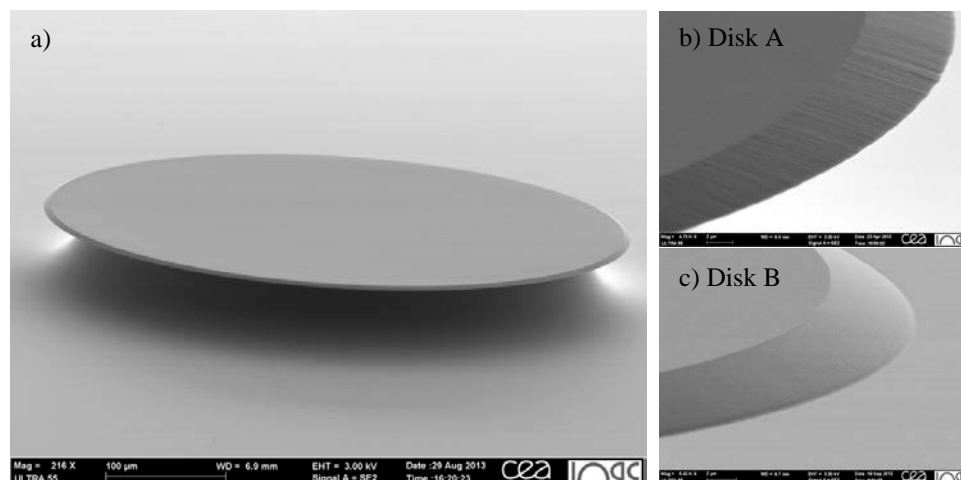
---

[a]Tassadit.Amrane@cea.fr

**Fig.1.** a) SEM picture of a 400 µm diameter SiO$_2$ microdisk; b) Disk A - roughness of a disk edge interface with standard fabrication process without roughness optimization steps; c) Disk B - roughness interface with specific process steps inspired from the Vahala group [10]
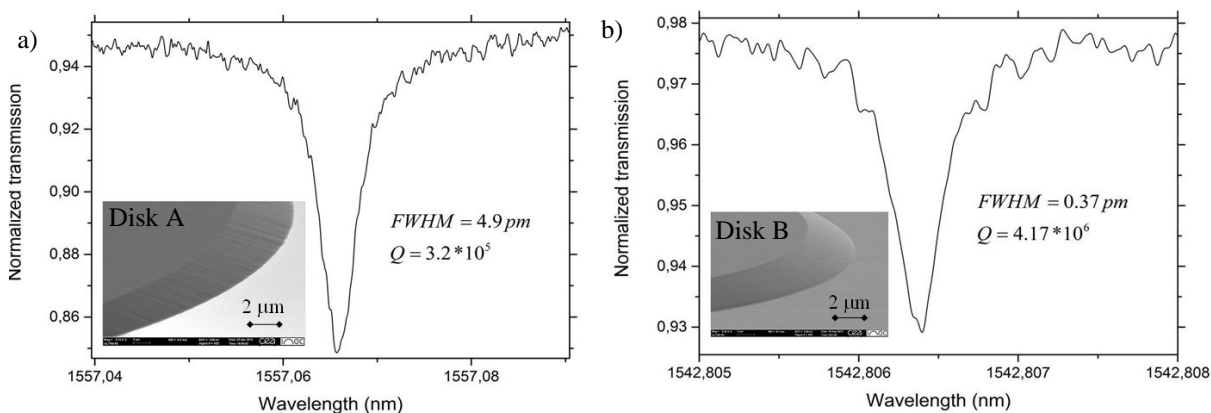


**Fig.2.** Transmission spectra across a WGM resonance for a) non optimized process on disk A b) roughness optimized fabrication process on disk B

The microresonators are characterized in the 1500 nm band: a tunable external cavity laser (linewidth 150 kHz, 1450-1590 nm) is connected to a tapered fiber and the transmitted signal is monitored with a low noise optical photodetector. The tapered optical fiber waveguide with a diameter of about 1-2 µm is realized by heating and stretching an optical fiber (SMF-28) and allows the light injection by evanescent coupling into the resonators placed on a piezoelectric three-axis stage. The resonances of the disks are efficiently excited by the tapered fiber and are detected by an absorption dip on the transmission spectrum. The experimental system is operated under N$_2$ atmosphere and optical measurements are performed in the under-coupling regime to limit the impact of the coupling losses. For each resonance, a quality factor can then be derived by measuring the resonance width. Examples of resonance and quality factor characterizations are given on Fig.2 a & b which correspond respectively to the previously detailed disks A and B from Fig.1.b and Fig.1.c: as expected, the roughness process improvement has a direct impact on the measured quality factor. Here an improvement by a factor of 10 is measured between the two realizations processes. Larger SiO$_2$ disks, with diameters up to 5 mm, have also been fabricated, and the highest quality factor $Q$ obtained to date with this process is of $6.5 \times 10^6$ for a 2 mm diameter disk as illustrated on Fig.3. The highest $Q \times D$ product obtained with these structures is currently of $1.3 \times 10^4$, which is in the range of the current state of the art for resonators used in IORG. Using these values and the parameters given in the Table 1, the actual ultimate minimal rotation resolution from Shot Noise contribution (2) is evaluated to only 125 °/h for our current setup. However, the fabrication process flow optimization is still under development in order to improve the resonators $Q$ factor and we estimate that $Q \times D$ product could be enhanced by several orders of magnitude for resonator diameters in the [1 mm-1 cm] range, which would translate into a minimum rotation rate resolution lower than 1 °/h.
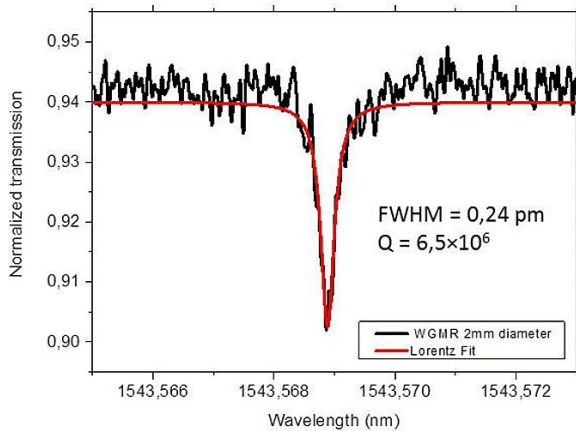
**Fig. 3.** Spectral response of a 2 mm diameter SiO2 microdisk realized with the optimized process flow

**Table 1.** Parameters for the Shot Noise resolution estimation in (2)

| Parameter | Value |
|---|---|
| Resonator diameter $D$ | 2 mm |
| Quality factor $Q$ | $6.5\times10^6$ |
| Measurement bandwidth $B$ | 1 Hz |
| Optical power at the photodetector $P$ | 1 mW |
| Photodetector efficiency $\eta$ | 0.74 |
| Laser central wavelength $\lambda$ | 1550 nm |

$$\delta\Omega_{Shot} = \frac{2c}{Q \times D} \times \sqrt{\frac{hcB}{\eta\lambda P}} \qquad (2)$$

III. DEVELOPMENT OF A SPECIFIC POLYMER PACKAGING

To ensure the mechanical stability of the optical coupling between the tapered fiber and the microresonator, a low refractive index polymer is used to encapsulate them: the optical system can thus be rotated without modification of its optical properties and a mechanical protection is provided to the sensing part. We have used a UV curable polymer, MY132A from MY Polymers Company, with a refractive index of 1.32 at 1550 nm which is low enough with respect to the $SiO_2$ one (1.44) to keep an efficient light confinement in the resonator. Few drops of polymer are spread on the sample in nitrogen environment to avoid oxygen contact and the device is then irradiated with UV light.

Fig.4 shows the spectral response obtained during the encapsulation process with the polymer for a given $SiO_2$ microresonator. On this example a reduction of the quality factor is observed, as it has been similarly observed in [12-14]. This result was expected as the penetration depth of the evanescent field outside the tapered fiber, given by $d = \lambda/(2\pi(n_r^2 - n_s^2)^{1/2})$, where $n_r$ and $n_s$ are respectively the resonator and the surrounding refractive indexes, is now reduced due to the polymer coating and the resonance modes in the resonator are more affected by the interface quality and defects.
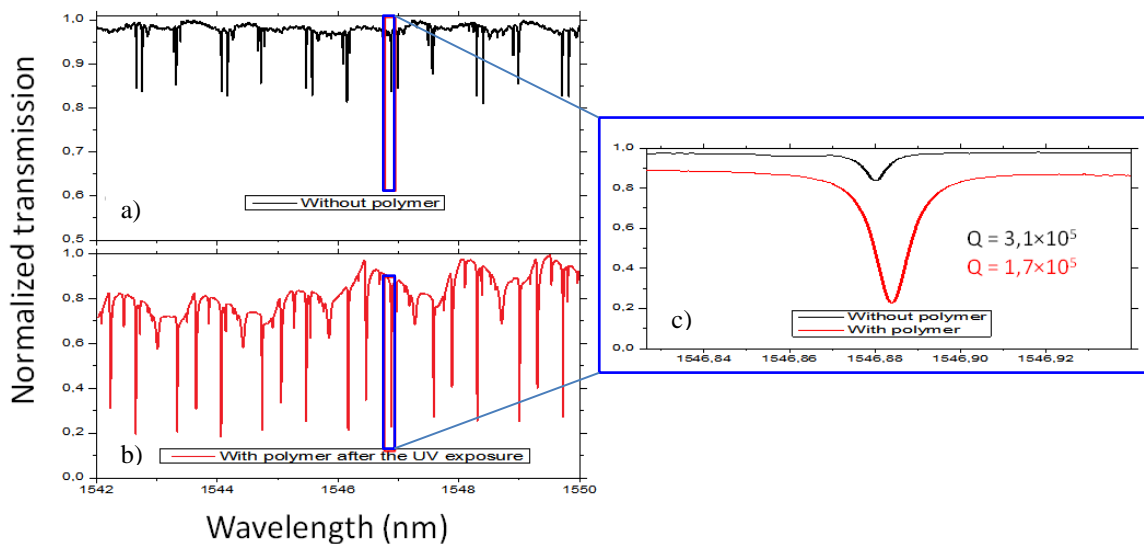


**Fig.4**. Spectral transmission of a $SiO_2$ microdisk before a) and after b) the polymer encapsulation, c) zoom on a resonance peak

IV. SYSTEM SETUP AND FIRST CHARACTERIZATIONS

In IORG the rotation rate measurement is achieved through the measurement of the Sagnac frequency shift occurring between the spectrum signature characteristics with light injected in the resonator in Clock-Wise (CW) and Counter Clock-Wise (CCW) directions [3][4][15]. To get first CW and CCW signal characterizations we have built a first test set-up around the $SiO_2$ microdisks detailed on Fig.5. The CW and CCW signals are injected from the laser source in the resonator with a 50/50 coupler connected to the tapered fiber and collected at the output of the resonator thanks to two circulators (C1/C2). Output signals are then analyzed on two low noise photodetectors (PD1/PD2). In order to characterize the CW and CCW resonance signals and then to lock on them, the laser wavelength has been modulated with an additional signal generator connected to the laser driver input, and response signals are demodulated at the output of the photodetectors with two lock-in amplifiers.

First, CW and CCW spectrum simultaneous characterizations at rest without modulations are detailed on Fig.6.a. for a large wavelength scan (8 nm) : the CW spectral response (black curve) perfectly matches the CCW one (red curve). A special care has to be taken of the different connections and interfaces to avoid any additional interference between CW and CCW signals. The intrinsic CW and CCW rotation sensitivity is then derived from a single peak scan performed over 50 pm at low frequency (50 mHz triangular ramp) with an additional modulation signal (500 Hz) for both CW and CCW lightwaves as illustrated on Fig.6.b.: the spectral responses for a given resonant peak are presented for modulated CW (green) and CCW (magenta) signals as well as for demodulated ones (CW (blue) and CCW (yellow)). The achieved rotation rate sensitivity is here in the range of 5-60 Hz/°/s for $SiO_2$ microdisks with diameter from 500 µm to 5 mm, with a corresponding scale factor of 0.2 µV/Hz to 2 µV/Hz for disk factor quality in the $10^5$-$10^6$ range for the current non-optimized lock-in amplifiers settings. All these figures could be improved by several orders of magnitude with better resonator quality factors and specifically optimized electronics.
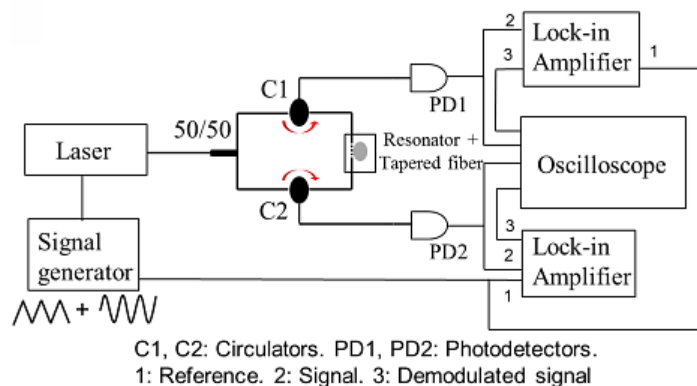


C1, C2: Circulators. PD1, PD2: Photodetectors.
1: Reference. 2: Signal. 3: Demodulated signal
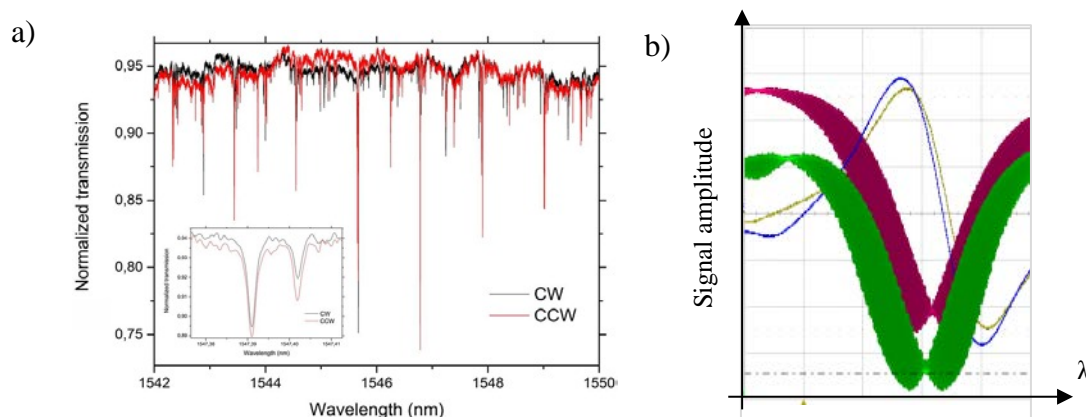
**Fig.5.** First system test setup



**Fig.6**. a) The WGMR spectral response on 8 nm range scan for CW (black) and CCW (red) lightwaves. The inset is a zoom for the peaks at 1547.39 nm. b) Resonant peaks (green and magenta) and their respective demodulated signals (blue and yellow) over 50 pm scan for the CW and CCW excitations.

IV. CONCLUSION AND PERSPECTIVES

In this paper, we have detailed our work towards using $SiO_2$ microdisks WGMR structures as sensitive part of an IORG. The very attractive possibilities offered by these structures in terms of $Q \times D$ product has been detailed and preliminary adapted structures have been realized and characterized. Results at the state of the art for resonators currently used in IORG have already been obtained with a reduced footprint. On-going work on the fabrication process to set our resonators properties at a higher quality factor level by several orders of magnitude (in the $10^7$ to $10^9$ range for resonators with diameters from 1 to 10 mm) shall then offer us the possibility to operate the system with an increased performance level up to rotation rate resolution limits of 1 °/h and lower. On system side, the $SiO_2$ microdisks resonators have been successfully characterized and specifically packaged in a low refractive index polymer for an upcoming use and characterization on a rotation plate. First CW and CCW signals characterization results at rest have been provided with a first system test setup. Test setup modifications and specific on-going work on dedicated operation and modulation scheme will allow us to build step by step the control loops and the associated electronics needed to operate the system as a functional gyroscope. Special care will be dedicated to the system optimization in order to reduce the perturbation sources such as backscattering and polarization issues that impact both the measurement noise and drifts of IORGs.

REFERENCES

[1] Ezekiel S. and Balsamo S. R., "Passive ring resonator laser gyroscope," Appl. Phys. Lett. 30, 478 (1977).
[2] Arditty H. J. and Lefèvre H. C., "Sagnac effect in fiber gyroscopes," Opt. Lett. 6(8), 401-403 (1981).
[3] Meyers, R. E., Ezekiel S., Stowe D. W. and Tekippe V. J., "Passive fiber-optic ring resonator for rotation sensing," Opt. Lett. 8(12), 644-646 (1983).
[4] Armenise M. N., Ciminelli C., Dell'Olio F., and Passaro V. N., [Advances in Gyroscope Technologies], Springer, 35 (2010).
[5] Ma H., Zhang X., Jin Z., & Ding C. "Waveguide-type optical passive ring resonator gyro using phase modulation technique," Opt. Eng. 45(8), (2006).
[6] Mao H., Ma H., Jin Z., "Polarization maintaining silica waveguide resonator optic gyro using double phase modulation technique ", Optics Express vol.19, No.5, (2011).
[7] Suzuki K., Takiguchi K. and Hotate K., "Monolithically Integrated Resonator Microoptic Gyro on Silica Planar Lightwave Circuit," J. Lightwave Technol., 66-72 (2000).
[8] Suzuki K. and Hotate K., "Integrated Optical Ring-Resonator Gyro Using Silica Planar Lightwave Circuit", Proc. SPIE 3541, Fiber Optic and Laser Sensors and Applications, (1998).
[9] Feng L., Lei M., Liu H., Zhi Y. and Wang J., "Suppression of backreflection noise in a resonator integrated optic gyro by hybrid phase-modulation technology," Appl. Opt. 52(8), 1668-1675 (2013).
[10] Lee H., Chen T., Li J., Yang K. Y.l, Jeon S., Painter O., and Vahala K. J., "Chemically etched ultrahigh-Q wedge-resonator on a silicon chip", Nature Photonics, Vol. 6, pp. 369-373, 2012.
[11] Jager J. B., Calvo V., Delamadeleine E., Hadji E., Noé P., Ricart T., et al, "High-Q silica microcavities on a chip: From microtoroid to microsphere," Appl. Phys. Lett. 99 (18), (2011).
[12] Yan Y. Z., Ji Z., Yan S. B., Liu J., Xue C. Y., Zhang W. D., et al, "Enhancing the robustness of the Microcavity Coupling System," Chin. Phys. Lett. 28(03), (2011).
[13] Yan Y. Z., Yan S. B., Ji Z., Liu J., Xue C. Y., Zhang W. D., and Xiong J. J., "Humidity and particulate testing of a high-Q microcavity packaging comprising a UV-curable polymer and tapered fiber coupler," Opt. Commun. 285, 2189-2194 (2012).
[14] Monifi F., Ozdemir S. K., Friedlein J., Yang L., "Encapsulation of a fiber taper coupled microtoroid resonator in a polymer matrix", IEEE Photonics Technology Letters, Vol. 25, Issue 15, pp. 1458 - 1461 (2013)
[15] Sanders G. A., Prentiss M. G., and Ezekiel S., "Passive ring resonator method for sensitive inertial rotation measurements in geophysics and relativity", Optics Letters, Vol. 6, Issue 11, 569-571 (1981).